JOURNAL OF SOLID STATE CHEMISTRY 99, 85–94 (1992)

A Theoretical Investigation of the Electronic Structure and the Chemical Bonding for Perovskite-Type Ti_3AlN

D. VOGTENHUBER-PAWELCZAK AND P. HERZIG

Institut für Physikalische Chemie, Universität Wien, Währingerstrasse 42, A-1090 Vienna, Austria

DEDICATED TO PROFESSOR A. NECKEL ON THE OCCASION OF HIS 65th BIRTHDAY

Received September 23, 1991; in revised form December 30, 1991; accepted December 31, 1991

For cubic perovskite-type Ti_3AlN a self-consistent LAPW band-structure calculation has been performed. In the energy range of ca. 0.5 Ry below the Fermi energy, distinct regions of partly overlapping bands are observed which correspond to peaks in the total density of states (DOS) curve that are separated by relatively deep minima. The bottom part of the band complex is formed by a band originating from Al 3*s* states followed by three nitrogen 2*p* bands and by three bands which are found at energies near the highest peak in the occupied part of the DOS and which are caused by Al 3*p* states. Just below (and also above) the Fermi level Ti 3*d* states are found. An analysis of the bonding situation in this compound is performed in terms of local partial DOS, partial charges, and electron density plots. The main contributions to covalent bonding are due to Ti–Ti, Ti–Al, and Ti–N interactions. The results are discussed and compared with recent findings for an ordered model structure for $Ti_{0.75}Al_{0.25}N$ and for a hypothetical cubic structure for Ti_3Al.

Introduction

After the preparation of Ti_2AlN, the first compound in the ternary system Ti–Al–N, by Jeitschko *et al.* (*1*) in 1963, it took almost 20 years before two further ternary compounds were found by Schuster and Bauer (*2*). One is perovskite-type Ti_3AlN and the other is trigonal $Ti_3Al_2N_2$. In Ti_2AlN and Ti_3AlN the Al atoms have only Ti atoms but no N atoms as nearest neighbors.

Ti_3AlN was found to exist between 1000 and 1300°C (*2*). Until very recently (*3*) the stoichiometry of the compound was believed to be 3 : 1 : 1. This assumption was based on crystallographic arguments and it corresponds to the case where all octahedral voids are occupied by nitrogen atoms. However, the chemical analysis of perovskite-type samples recently prepared by Pietzka and Schuster (*3*) revealed a nitrogen content of 12.3 at.% equivalent to the composition of $Ti_3AlN_{0.5}$. A similar situation was observed for the corresponding carbide with an experimental carbon content of 12.7 at.% which leads to a 50% occupancy of the carbon sites. These new experiments (*3*) were performed in order to prepare samples for the measurement of thermochemical data in the quaternary system Ti–Al–C–N.

Different kinds of titanium aluminum ni-

0022-4596/92 $5.00

trides (*4–6*) have recently attracted considerable interest because of their exceptional properties as regards hardness, wear resistance, and resistance against oxidation at higher temperatures. They can be prepared in layers of up to 10 μm and form metastable phases. Their structure can be derived from TiN with sodium chloride structure by randomly replacing Ti atoms with Al atoms and their composition is given by $Ti_{1-x}Al_xN$ for $0 > x > 0.5$. In these compounds the Al atoms have N atoms as nearest neighbors and therefore Al tends to be relatively ionic.

After a recent theoretical investigation of those metastable phases based on ordered model structures for $Ti_{0.75}Al_{0.25}N$ and $Ti_{0.50}Al_{0.50}N$ (*7*), and also using the KKR-CPA method (*8, 9*), where the Ti and Al atoms are assumed to be randomly distributed over the metal lattice sites, the aim of the present paper is to study the perovskite-type compound Ti_3AlN. If one considers the phase diagram of the ternary Ti–Al–N system, Ti_3AlN lies on the line joining metallic Ti and insulating, ceramic AlN and is therefore an interesting candidate for a theoretical investigation.

The present calculation has been performed for the stoichiometric compound and the results can therefore be compared easily with those of the model structure Ti_3AlN_4 (*7*). There is a close relationship between the two structures: the unit cell of Ti_3AlN is obtained by the removal of three of the four N atoms of Ti_3AlN_4.

The results will also be compared with recent results (*10*) for the hypothetical cubic Cu_3Au ($L1_2$) structure of Ti_3Al. This structure yields that of Ti_3AlN, if a nitrogen atom is put in the center of the octahedron formed by titanium atoms.

In this context the recent publication by Ivanovskii *et al.* (*11*) shall be mentioned which investigates the electronic structure of perovskite-type titanium aluminum carbide and of several other related compounds.

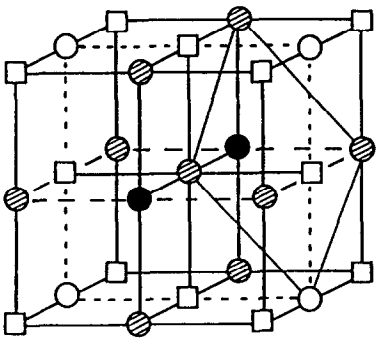

FIG. 1. Structure for Ti_3AlN. ●, N atoms; ◍, Ti atoms; ○, Al atoms; □, empty spheres; ···, (100) plane, cut 1; ——, (100) plane, cut 2; —, (111) plane.

Computational Aspects

An electronic band structure calculation using the self-consistent LAPW method (*12, 13*) and the Hedin–Lundqvist exchange-correlation potential (*14*) has been performed on Ti_3AlN crystallizing into the perovskite structure (Fig. 1). In order to avoid exceedingly large Al sphere radii, empty spheres (in the following text designated as □) were used in the calculation (see Fig. 1), the radii of which are equal to the radii of the N spheres. The atomic sphere radii for Ti and N were chosen such that their ratio is the same as for TiN (*15*). The sphere radius for Al is identical to that for Ti. The muffin-tin radii were kept constant during the SCF cycles. The lattice parameter, which has been chosen according to Schuster and Bauer (*2*), and the muffin-tin radii are given in Table I.

The site symmetry for the three Ti atoms and the three empty spheres in the unit cell is D_{4h}, and for the single Al and the single N atom O_h. For the designation of the Ti d components an internal coordinate system has been defined in which the z axis points towards the adjacent N atom.

Because of the high symmetry of the crystal structure the muffin-tin approximation for the potential seems to be justified. For

TABLE I

INPUT DATA (IN a.u.)

Lattice constant		7.770557
Muffin-tin radii	Ti, Al	2.06390
	N, □	1.82138

the electron density, however, the more general warped muffin-tin approximation has been used, i.e., the electron density between the atomic spheres was expressed as a Fourier series.

For Ti, the 1*s*, 2*s*, and 2*p* states, for Al the 1*s* and 2*s* states, and for N the 1*s* states were treated as core states and all the other states as band states.

The starting potentials were obtained by a superposition of the electron densities of the neutral atoms, for which Poisson's equation was solved.

A maximum of 480 **k** vectors were taken in the **k** expansion of the wave function, while the l expansion inside the muffin-tin spheres was extended up to $l = 12$.

For the selfconsistency procedure, 10 **k** points in the irreducible part of the Brillouin zone were chosen. Thereafter one iteration with 165 **k** points was performed to get an accurate band structure and DOS. For plotting the band structure, the irreducible representations to which the eigenstates belong were evaluated from the eigenvectors in order to fulfill the compatibility relations.

The total and partial DOS were calculated using the tetrahedron method by Lehmann and Taut (*16*). Although the present calculation was based on unsymmetrized basis functions, the formalism given in (*17*) for the computation of the electron densities was used.

Results

(*a*) *Band Structure and DOS*

The band structure of the valence bands of Ti_3AlN is shown in Fig. 2. In the energy region between −0.31 and −0.20 Ry a single band originating from the N 2*s* states appears that is denoted as "*s* band." The corresponding peak in the total DOS (see Fig. 3) is almost completely dominated by the N *s* partial DOS with small Ti d_{z^2} contributions at lower energies and Ti p_z contributions at the high-energy edge of the band.

The nitrogen "*s* band" is separated from the other bands at higher energies by a gap of 0.47 Ry (exact band-structure data can be taken from Table II).

The following four bands, up to an energy of 0.55 Ry, are caused by N 2*p* and Al 3*s* states ("N *p* band"). For most of the **k**

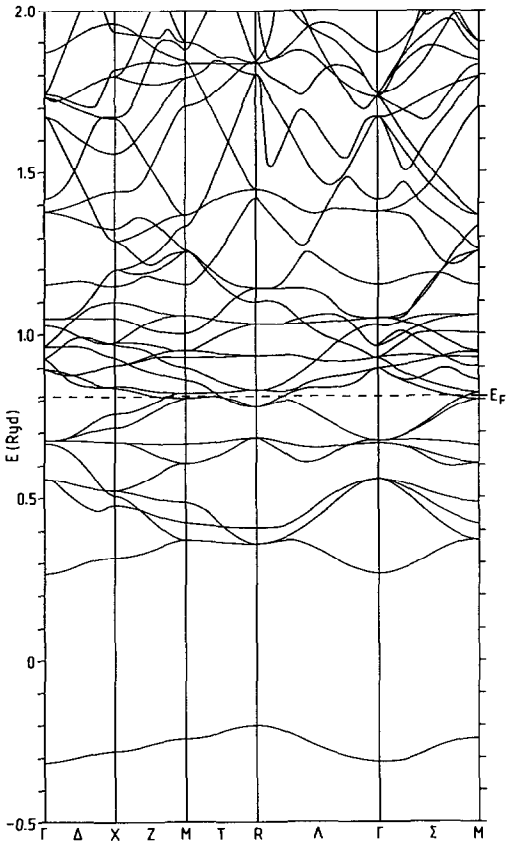

FIG. 2. Band structure of Ti_3AlN. Energies with respect to the constant muffin-tin potential between the spheres.

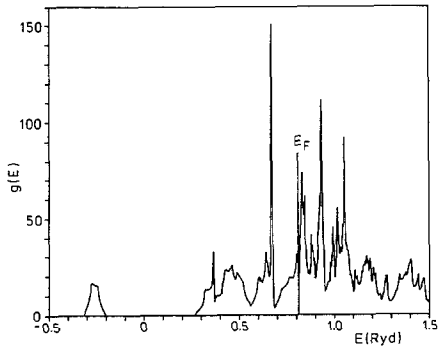

FIG. 3. Total DOS for Ti_3AlN in units of states per Ry per spin and per unit cell.

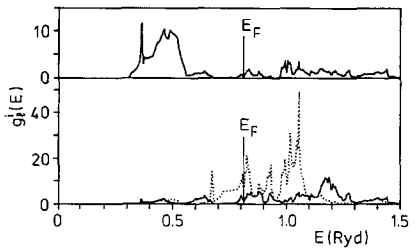

FIG. 4. Local partial DOS of components showing N–Ti interaction (the same units as in Fig. 3 are used). Top: N p DOS. Bottom: Ti d_{z^2} (——) and Ti (d_{xz}, d_{yz}) (···) DOS.

points the Al s band lies below the N p bands. However, it crosses the N p bands and is found above them near the **k** points M and R.

The next band after a pseudogap is the "Al p band". It consists of three rather flat bands between 0.55 and 0.69 Ry and, at the **k** point Γ, overlaps with the "d band," a complex of 15 bands originating from Ti $3d$ states and extending to an energy of 1.28 Ry which is far above the Fermi level at 0.815 Ry.

When the band structure of Ti_3AlN is compared with the one for the model structure of $Ti_{0.75}Al_{0.25}N$ (7), the most significant differences, apart from the smaller number of bands in Ti_3AlN due to the smaller number of atoms in the unit cell, are on the one hand the larger width of the band gap between the "s band" and the "(N) p band" brought about by the absence of covalent Al–N s–p interactions, and on the other hand the appearance of the "Al p band" in an energy region of a relatively low DOS in Ti_3AlN_4.

TABLE II

BAND STRUCTURE DATA FOR Ti_3AlN (IN RY)

	Band	E
Band width	s	0.111
	N-p	0.272
	Al-p	0.147
	Occupied d	0.129
Band gap	s-Np	0.470
E_F (with respect to bottom of s band)		1.128
E_F (with respect to bottom of N-p band)		0.547
E_F (with respect to muffin-tin zero)		0.815

The classification in four regions of "bands" introduced above is also useful in the discussion of the total DOS (Fig. 3). There are a gap between the "s band" and the "N p band" and deep minima at 0.55 and 0.69 Ry, which separate the "N p band" from the "Al p band" and the latter from the "d band". The Fermi level lies in a local minimum. Integration of the DOS over the four energy regions gives the number of accommodated electrons as 2, 8, 6, and 4, respectively.

Figures 4–6 show the various local partial DOS components, whereby the components involved in particular types of bonds are collected in corresponding figures.

In the lower part of the "N p band," up to an energy of ca. 0.4 Ry, the main component is the one with the N p character. The presence of Ti d_{z^2} and (d_{xz}, d_{yz}) contributions shows that covalent Ti–N d–p σ and π bonds occur in this energy range. Apart

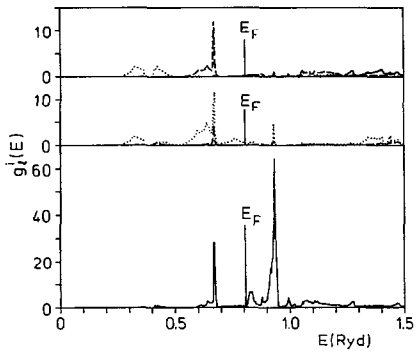

FIG. 5. Local partial DOS of components involved in Ti–Al and in Al–Al bonds (the same units as in Fig. 3 are used). Top: Al s (···) Al p (---), and Al d (——) DOS. Center: □ s (···) and □ p_z (---) DOS. Bottom: Ti d_{xy} DOS.

from the Ti–N interactions, relatively large s partial DOS components in the Al and empty spheres also indicate the importance of Al–Al s–s σ interactions across the empty spheres.

The situation in the upper part of the "N p band" is slightly more complicated due to the additional appearance of Ti d_{xy} and □ p_z peaks in the local partial DOS. They can be understood by the presence of states which do not have a node in the Al sphere (s-like character) and which form Ti–Al d–s σ bonds and also Ti–Ti d–d π bonds across the empty spheres.

In the "Al p bands," the most striking difference compared to the "N p band" is that the Al character is almost exclusively

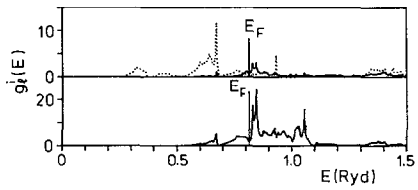

FIG. 6. Local partial DOS of components showing Ti–Ti interaction across the empty spheres (the same units as in Fig. 3 are used). Top, □ s (···) and □ (p_x, p_y) (——) DOS. Bottom, Ti $d_{x^2-y^2}$ DOS.

p-like. There is still some Ti–N σ and π bonding, but the bonding situation between the metal atoms has changed. There are now Ti–Al d_{xy}–p σ bonds and the Ti $d_{x^2-y^2}$ partial DOS component indicates the existence of Ti–Ti d–d σ bonds across the empty spheres. The p character in the Al sphere requires one nodal plane of the wave function which, for states having the Ti d_{xy} character, leads to energetically less favorable Ti–Ti d–d δ bonds.

The states in the occupied part of the "d band" mainly contribute to the Ti–Ti d–d σ bonding. The largest partial DOS component for Ti is the (d_{xz}, d_{yz}) component which is involved in the σ bonds between the six Ti atoms octahedrally surrounding the N atoms. The other important type of Ti–Ti bond is due to the interaction of the $d_{x^2-y^2}$ orbitals which, for the bonding interaction, leads to s-like DOS in the empty sphere.

(*b*) *Charge Transfer and Partial Charges*

The bottom part of Table III shows the differences between the self-consistent LAPW charges and the superposed charges of the neutral atoms (charge transfer) for the muffin-tin spheres and the interstitial region of Ti_3AlN. These results shall be compared with the corresponding results for the model structure Ti_3AlN_4 (*7*) and also for TiN (*15*). In all these compounds there is a charge transfer from the titanium sphere to the nitrogen sphere. While for the nitrogen sphere the charge differences are roughly the same in all three cases (ca. 0.37 electrons per muffin-tin sphere), the value for the titanium sphere is much lower for the perovskite structure than for TiN and Ti_3AlN_4. Similar but even more pronounced effects are observed if the charge transfer for the aluminum sphere of Ti_3AlN is compared with the corresponding quantity for Ti_3AlN_4. These findings and the opposite charge transfer in the interstitial region reflect the completely different bonding situations for the two titanium nitrides, i.e., the considerably reduced

TABLE III

PARTIAL CHARGES FOR Ti_3AlN (IN ELECTRONS PER ATOMIC SPHERE)

Band		Ti	Al	N	□	PW
s	*s*	0.01	—	1.49	—	
	p	0.01	—	—	—	
	d	0.02	—	—	—	
	Total	0.05	—	1.50	—	0.35
N-*p*	*s*	0.07	0.44	0.02	0.12	
	p	0.07	0.04	2.80	0.03	
	d	0.33	—	—	—	
	Total	0.48	0.49	2.83	0.16	2.77
Al-*p*	*s*	0.02	0.02	—	0.26	
	p	0.04	0.44	0.25	0.05	
	d	0.57	0.01	0.02	0.01	
	Total	0.64	0.48	0.27	0.32	2.36
Occupied *d*	*s*	—	—	—	0.06	
	p	0.01	0.01	0.06	0.03	
	d	0.79	0.03	0.03	0.01	
	Total	0.81	0.04	0.10	0.10	1.13
Occupied valence	*s*	0.11	0.46	1.52	0.44	
	p	0.14	0.50	3.12	0.11	
	d	1.71	0.04	0.05	0.02	
	Total	1.98	1.01	4.70	0.58	6.61
Charge differences		−0.18	−0.17	0.37	0.03	0.24

Note. Charge differences are taken between total selfconsistent LAPW charges and atomic superposed charges.

ionicity of the metal atoms in the perovskite-type compound due to the much smaller number of nitrogen atoms as compared to the model structure Ti_3AlN_4.

In the upper part of Table III the partial charges obtained by summing the *local* partial charges over the energy ranges of the "*s*," "N *p*," "Al *p*," and the occupied part of the "*d* band" are given. For a comparison with the partial charges of Ti_3AlN_4 see Table III of (*7*). All charges refer to a single muffin-tin sphere and to the whole of the interstitial volume, except for the data for Ti_3AlN_4 which refer to only a quarter of the interstitial volume. The split of the Ti 3*d* charges into their components in a crystal field of D_{4h} symmetry is presented in Table IV.

In the "*s* band" the situation is very much the same as in Ti_3AlN_4, except for the Al partial charges which are all zero in the perovskite-type compound, because there are no Al atoms next to the N atoms, and the interstitial charge which is just a quarter of the Ti_3AlN_4 case.

In the region of the "N *p* band" a band caused by the Al 3*s* states is found also. The

TABLE IV

SPLIT OF THE Ti-*d* PARTIAL CHARGES (IN ELECTRONS PER MUFFIN-TIN SPHERE)

Band	d_{z^2}	$d_{x^2-y^2}$	d_{xy}	(d_{xz}, d_{yz})
s	0.02	—	—	—
N-*p*	0.13	—	0.03	0.17
Al-*p*	0.14	0.10	0.22	0.11
Occupied *d*	0.06	0.20	0.06	0.47
Occupied valence	0.35	0.31	0.31	0.75

partial charges reflect the bonding situation in this energy range: Ti–N d–p σ and π bonds as well as Al $3s$ states which have mainly s character in the empty sphere. Compared to Ti_3AlN_4 the main differences concern the Al partial charges and the much smaller Ti d charge because of the drastically reduced number of Ti–N bonds.

The partial charges of the "Al p band" suggest the importance of Ti–Al d–p σ interactions and also Ti–N d–p σ interactions in this band.

Compared to TiN, in the occupied "d band" there is considerably more charge in Ti d states and in the interstitial region compensating the reduced number of N atoms and their much smaller d band partial charge.

(c) *Electron Density and Chemical Bonding*

Figure 7 shows the valence electron density of Ti_3AlN for the two inequivalent cuts in the (100) plane marked in Fig. 1. The maxima inside the Ti spheres point towards the empty sphere (cut 1) and towards the neighboring Ti atoms (cut 2) thus indicating the two important types of covalent bonding in this compound, i.e.,Ti–Ti bonds via the empty sphere and Ti–Ti bonds between neighboring atoms.

A more detailed analysis can be performed if the electron density contributions of the "N p band," the "Al p band," and of the occupied "d band" are considered separately (Fig. 7). Cut 2 of the electron density of the "N p band" clearly illustrates the Ti–N d–p σ bonds while cut 1 reveals the interaction of the Ti d_{xy} states with the Al s states forming d–s σ bonds.

Cut 1 of the "Al p band" electron density shows the Ti–Al d–p σ bonds caused by the interaction of Ti d_{xy} and Al p states. The Ti–N d–p σ bonds are not only observed in the "N p band" but also in the energy region of the "Al p band" (cut 2).

In the occupied part of the "d band," where almost exclusively Ti–Ti bonds are found, Ti–Ti $d_{x^2-y^2}$–$d_{x^2-y^2}$ σ bonds (cut 1) and (d_{xz}, d_{yz})–(d_{xz}, d_{yz}) σ bonds (cut 2) can be identified.

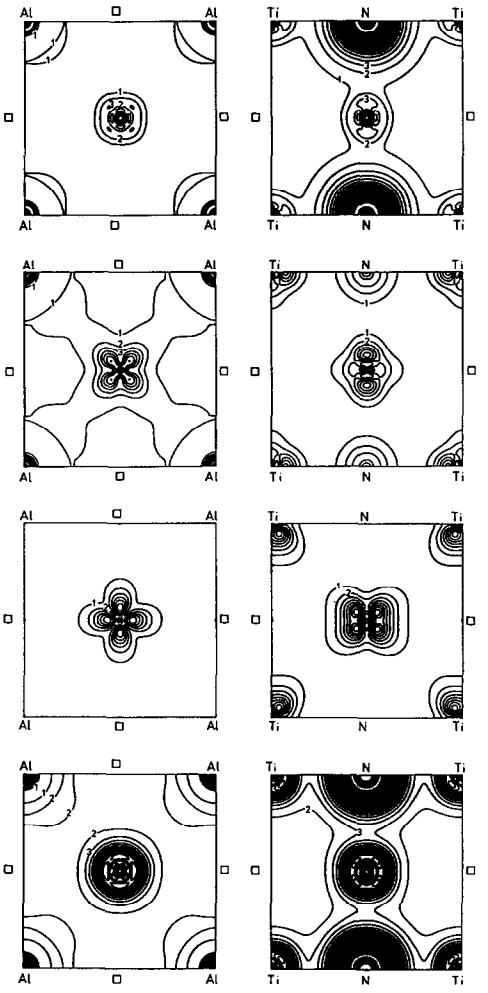

FIG. 7. Electron densities of the various "bands" in units of 10^{-1} eÅ^{-3}. Left columns: (100) plane, cut 1; right columns: (100) plane, cut 2. Top row, "N p band"; second row, "Al p band"; third row, occupied part of the "d band"; bottom row, total valence electron densities.

In Fig. 8 the electron density of the "Al p band" and the total valence electron density in the (111) plane are shown. In the first plot, where the maxima of the electron

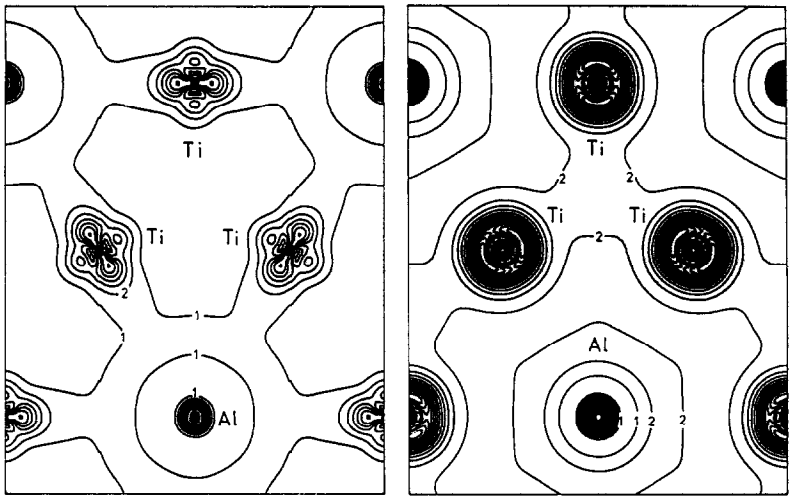

Fig. 8. Electron densities in the (111) plane in units of 10^{-1} eÅ^{-3}. Left: "Al p band," right: total valence electron density.

density about the Ti atoms are directed towards the Al atoms, the Ti–Al d_{xy}–p σ bonds can be seen. The ring-shaped maxima around the Al atoms are caused by the Al $3p$ orbitals.

In the valence electron density in the (111) plane the maxima of the Ti electron density point towards the centers of the triangles formed by the Ti atoms where a flat density maximum is observed. This behavior results from the superposition of the electron density contributions of the various bonds including the bonds towards the nitrogen atoms above (or below) the Ti triangles.

For a comparison of the relative bond strengths between the perovskite structure, Ti_3AlN, and the model structure, Ti_3AlN_4, it is useful to consider the density difference plots for the two cuts in the (100) plane (Fig. 9) where the valence electron density (without the contribution of the "s band") of Ti_3AlN_4 is subtracted from the corresponding density of Ti_3AlN.

Cut 1 shows a positive difference of the electronic charges at the Ti and Al atoms and also between these two atoms. These findings suggest a reduced ionicity and an increase in the covalent character of the Ti–Al bonds. The maxima of the electron density difference around Ti directed toward the empty spheres in Ti_3AlN (and the $N^{[4]}$ spheres in Ti_3AlN_4) lead to the conclusion that the Ti–Ti d–d σ bonds across the vacancy are at least of comparable strength to the Ti–$N^{[4]}$ bonds in Ti_3AlN_4.

Inspection of cut 2 of the electron density difference plots mainly reveals the strengthening of the Ti–N bonds compared with the Ti–$N^{[6]}$ bands in Ti_3AlN_4.

Conclusions

The results of the present investigation can be summarized as follows:

The calculated band structure shows that Ti_3AlN behaves as a metal.

In the DOS characteristic peaks are observed which correspond to distinct regions of "bands" in the band structure. Those "bands" are related to the different types of covalent bonds in Ti_3AlN. The Ti–N d–p σ and Al–Al s–s and p–p σ bonds are observed mainly in the "N p" and "Al p band," the Ti–Al d–p σ bonds in the "Al p

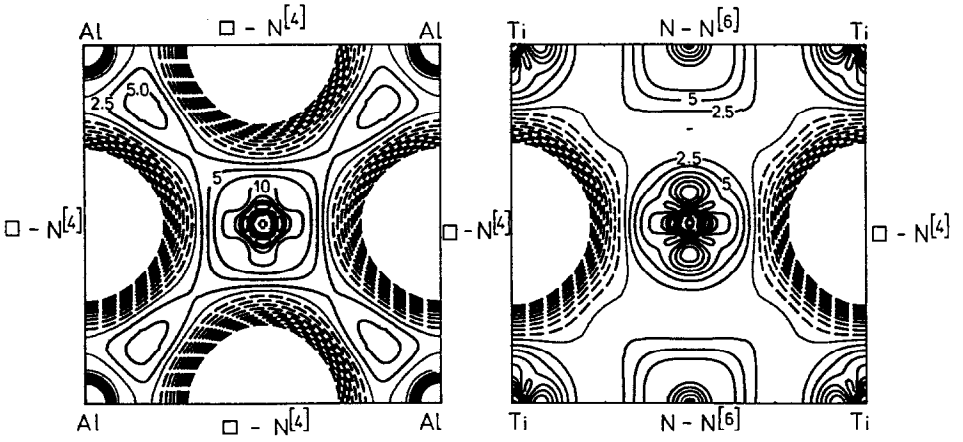

FIG. 9. Difference electron densities of the valence bands (omitting the "*s* band") in the (100) plane, cuts 1 (left) and 2 (right) in units of $10^{-2}\ e\text{Å}^{-3}$.

band," and the Ti–Ti d–d σ bonds in the "*d* band."

As regards the stability of the compound, the covalent Ti–Ti bonds seem to be of crucial importance. Apart from the d–d σ and π interactions of neighboring Ti atoms, the $d_{x^2-y^2}$–$d_{x^2-y^2}$ σ interactions also form strong covalent bonds which are mainly caused by states in the "Al *p* band." This can be deduced from the high □ *s* character in that energy region (Fig. 6).

The comparison of the results for Ti_3AlN with those for the ordered model structure for $Ti_{0.75}Al_{0.25}N$ shows a reduced ionicity and an increased strength of the covalent bonding in Ti_3AlN. However, due to the smaller number of nitrogen atoms in Ti_3AlN, the importance of Ti–N bonding is greatly reduced. Nevertheless, the presence of nitrogen is indispensable for the stability of the phase, as cubic Ti_3Al (Cu_3Au structure) does not exist. A recent investigation of this hypothetical cubic structure for Ti_3Al (*10*) reveals that the electron density in the (111) plane is very similar to that of Ti_3AlN (Fig. 8). The most striking difference is a slightly higher electron density in the centers of the Ti triangles in Ti_3AlN caused by the presence of nitrogen atoms.

Assuming a rigid band model the following can be deduced from the present calculation for the experimentally observed nonstoichiometric composition of $Ti_3AlN_{0.5}$. The Fermi energy would be lowered by about 0.03 Ry whereby the DOS at the Fermi level would be slightly reduced. Considering the bonds that are formed by states in this energy region, i.e., mainly Ti–Ti $d_{x^2-y^2}$–$d_{x^2-y^2}$ σ bonds across the empty sphere and Ti–Ti (d_{xz}, d_{yz})–(d_{xz}, d_{yz}) σ bonds, the former are antibonding, as can be seen from the *p*-like charge in the empty sphere, while a similar classification for the latter bonds cannot be made from the available results.

Acknowledgments

We are grateful to the Austrian Fonds zur Förderung der wissenschaftlichen Forschung for financial support (Project 7117) and to Dr. J. C. Schuster for helpful discussions. The calculations were performed on an IBM 3090-400E VF at the Computing Center of the University of Vienna under the European Academic Supercomputing Initiative (EASI).

References

1. W. JEITSCHKO, H. NOWOTNY, AND F. BENESOVSKY, *Monatsh. Chem.* **94,** 1198 (1963).

2. J. C. SCHUSTER AND J. BAUER, *J. Solid State Chem.* **53,** 260 (1984).
3. M. PIETZKA AND J. C. SCHUSTER, "COST 507 Status Seminar, Leuven, Belgium, Dec. 1991."
4. H. A. JEHN, S. HOFMANN, V. E. RÜCKBORN, AND W. D. MÜNZ, *J. Vac. Sci. Technol. A* **4,** 2701 (1986).
5. O. KNOTEK, M. BÖHMER, AND T. LEYENDECKER, *J. Vac. Sci. Technol. A* **4,** 2695 (1986).
6. W. D. MÜNZ, *J. Vac. Sci. Technol. A* **4,** 2717 (1986).
7. D. VOGTENHUBER-PAWELZCAK, P. HERZIG, AND J. KLÍMA, *Z. Phys. B Condens. Matter* **84,** 211 (1991).
8. J. PETRŮ, J. KLÍMA, AND P. HERZIG, *Z. Phys. B Condens. Matter* **76,** 483 (1989).
9. L. SZUNYOGH, J. KLÍMA, D. VOGTENHUBER-PAWELCZAK, P. HERZIG, AND P. WEINBERGER, *Z. Phys. B Condens. Matter* **85,** 281 (1991).
10. T. HONG, T. J. WATSON-YANG, X. Q. GUO, A. J. FREEMAN, T. OGUCHI, AND J. XU, *Phys. Rev. B, Condens. Matter* **43,** 1940 (1991).
11. A. L. IVANOVSKII, V. I. ANISIMOV, I. V. SOLOV'EV, YU. G. ZAINULIN, AND V. A. GUBANOV, *Izv. Akad. Nauk SSSR, Neorg. Mater.* **24,** 1311 (1988); *Inorg. Mater.* **24,** 1120 (1988).
12. O. K. ANDERSEN, *Phys. Rev. B, Condens. Matter* **12,** 3060 (1975).
13. D. D. KOELLING AND G. O. ARBMAN, *J. Phys. F* **5,** 2041 (1975).
14. L. HEDIN AND S. LUNDQVIST, *J. Phys. (Paris)* **33,** C3–73 (1972).
15. P. HERZIG, J. REDINGER, R. EIBLER, AND A. NECKEL, *J. Solid State Chem.* **70,** 281 (1987).
16. G. LEHMANN AND M. TAUT, *Phys. Status Solidi B* **54,** 469 (1972).
17. J. REDINGER, R. EIBLER, P. HERZIG, A. NECKEL, R. PODLOUCKY, AND E. WIMMER, *J. Phys. Chem. Solids* **47,** 387 (1986).